

Spectroscopy of a ferroelectric plasma cathode

A. Dunaevsky, K. Chirko, Ya. E. Krasik,^{a)} and J. Felsteiner
Department of Physics, Technion, 32000 Haifa, Israel

V. Bershtam
Department of Physics, Weizmann Institute of Science, 76100 Rehovot, Israel

(Received 11 June 2001; accepted for publication 24 July 2001)

Results of spectroscopic investigations of the plasma formed on the surface of a ferroelectric cathode upon the application of a driving pulse are presented. The ferroelectric plasma cathode was made of a solid solution of Sr, Ba, Ti, Nb, Pb, and O. Its front side was covered by Cu grounded strip electrodes. A driving pulse with an amplitude ≤ 18 kV and pulse duration of ~ 400 ns was applied to the rear Cu disk electrode. A Jobin-Yvon 750M spectrometer was used for visible light dispersion. Spectral line profiles were obtained by a fast framing camera. It was shown that light is emitted from the excited ions and neutral atoms of Cu, Pb, Sr, Ba, Ti, and H within the first 50 ns after the beginning of the driving pulse. By analyzing the Doppler broadening of the observed spectral line profiles it was found that the ion and neutral atom temperature is ≤ 0.8 eV. Analysis of the Stark broadening of the H_α and H_β spectral lines showed the absence of a high (> 1 kV/cm) electric field which could be developed at the surface of the ferroelectric due to the appearance of noncompensated surface polarization charges. The same Stark analysis also showed that the plasma density does not exceed 10^{13} cm⁻³. By comparing the relative intensities of the H_α and H_β spectral lines obtained with the results of collision radiative modeling, the plasma electron temperature was found to be ~ 3 eV. © 2001 American Institute of Physics. [DOI: 10.1063/1.1404421]

I. INTRODUCTION

Recent investigations of ferroelectric cathodes have showed that they can be used for the generation of high-current electron beams with current amplitudes of several kA, electron energies of several hundred keV, and pulse duration of several hundred ns.¹⁻⁵ The main advantages of ferroelectric cathodes compared to explosive emission cathodes⁶ are their capability to generate electron beams at relatively small accelerating voltages without a time delay with respect to the beginning of the accelerating pulse and to keep quasicontant diode impedance.⁷

In earlier publications, the unusual emission properties of ferroelectric cathodes were explained by the model of polarization reversal.^{5,8} This model is based on a nanosecond scale polarization reversal of a preliminary polarized ferroelectric sample. It is assumed that fast polarization reversal occurs upon the application of a driving pulse, with appropriate polarity and amplitude, between ferroelectric sample electrodes. The process of polarization reversal leads to the appearance of a noncompensated negative polarization surface charge density $\sigma = 2P_s$ (here P_s is spontaneous polarization of the ferroelectric) at the front surface of the ferroelectric. This charge is responsible for an extremely large normal component of the electric field ($E \sim 10^7 - 10^8$ V/cm) which causes the observed copious electron emission. This type of emission is referred to as ferroelectric emission. However, this model failed to explain experimental data which showed that the observed copious emission occurs

also above the Curie temperature of the ferroelectric tested, or when the driving pulse cannot produce reversal polarization.⁵ Also, the assumption of polarization reversal on a nanosecond time scale for thick ferroelectrics (several mm in thickness) is doubtful.⁵ We note that simultaneous with the appearance of the electric field which has a normal component with respect to the front surface of the ferroelectric, a tangential component near the edge of the front electrode should appear as well. This tangential component should cause a surface flashover with corresponding plasma formation at electric fields of $10^4 - 10^5$ V/cm.⁵

It has recently been shown⁹⁻¹³ that the source of the observed copious electron emission is a plasma which is formed on the surface of the ferroelectric cathode as a result of surface flashover initiated in triple points.^{14,15} It was claimed that the application of the driving pulse leads to the appearance of noncompensated surface polarization charge in these locations. The appearance of this charge could be either due to a regular polarization process of a nonpolarized ferroelectric or a linear dielectric or due to a noncomplete switching process in the case of a preliminarily polarized ferroelectric. This polarization charge is responsible for enhancement of the electric field in the triple points followed by field or explosive electron emission in these locations. Further, due to the existence of a tangential component of the electric field¹¹ electron avalanching occurs along the surface of the ferroelectric which leads to surface plasma formation.¹⁶ This plasma covers the surface of the ferroelectric, serving as a dynamic electrode. Thus, the plasma provides charged particles for screening of the surface polarization charge.

^{a)}Electronic mail: fnkrasik@physics.technion.ac.il

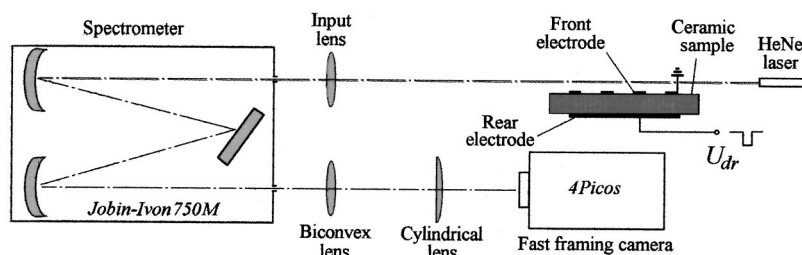


FIG. 1. Experimental setup.

Ferroelectric samples with different compositions (TGS, PLZT, PZT, and BaTiO_3) and different polarization states were used in these experiments.⁵ Using framing photography it was shown that the light emission from the front surface of all the samples appears within the first 50 ns with respect to application of the driving pulse. It was believed that the observed light emission occurs from the surface plasma.¹² The parameters of the plasma were studied by different electric probes (floating single and double Langmuir probes, biased collimated Faraday cups, electrostatic spectrometer, etc.).¹³ These studies showed that the parameters of the plasma depend strongly on the amplitude and polarity of the driving pulse as well as on the composition of the ferroelectric sample. However, all the above methods for measuring the plasma parameters were either indirect (visible light observation) or disturbing methods (electric probes). Also, we note that the authors of some recent publications^{17–20} continue to claim that the source of the observed electron emission is not the surface discharge plasma but pure ferroelectric emission.

In this article, we present results of spectroscopic investigation of the plasma formed on the surface of the ferroelectric sample upon the application of a driving pulse. Spectroscopic measurements are a nondestructive method that allows determination of basic plasma parameters (plasma ion and electron temperature and plasma density) by analyzing the different emission spectral line profiles. We note that visible light spectroscopy was used in previous research related to the investigation of surface flashover in the triple points.^{21,22} It was shown that intense line emission of different excited neutral atoms and ions appears almost simultaneously with the application of a high-voltage nanosecond driving pulse to the electrode attached to the BaTiO_3 surface.

In the present experiments the plasma ion temperature was determined by analyzing the Doppler broadening of different spectral line profiles. The upper boundary of the plasma electron density was estimated by the Stark broadening of the H_α and H_β spectral lines. By comparing the observed relative intensities of the H_α and H_β spectral lines with results of collision radiative modeling the electron temperature was obtained. The observed data showed that application of the driving pulse causes intense plasma formation and that this plasma consists of neutrals and ions whose origin is the electrode and sample material.

II. EXPERIMENTAL SETUP

The experimental setup is shown in Fig. 1. The ferroelectric cathode was of disk form with a diameter of 137 mm and a thickness of 8 mm. Its composition was determined by x-ray diffraction to be a solid solution of $\text{Pb}_{0.7}\text{Ba}_{0.3}\text{Nb}_2\text{O}_6$,

$\text{Sr}_{0.5}\text{Ba}_{0.5}\text{Nb}_2\text{O}_6$, $\text{Sr}_2\text{Ba}_4\text{Ti}_2\text{Nb}_8\text{O}_{30}$, and $\text{Ba}(\text{Pb}_{0.33}\text{Nb}_{0.67})\text{O}_3$. This composition showed a longer lifetime compared with other ferroelectric ceramics, namely, PZT and PLZT.²³ We believe that the present results are also relevant for other ferroelectric compositions. In fact, light emission and plasma formation were observed with different ferroelectric ceramics independent of their composition and polarization state.^{5,12,13}

The ceramic sample was covered by a copper front electrode in the form of strips. The diameter of the surface area covered by strips was 70 mm. The front electrode was glued to the ceramic surface by conducting glue. A solid rear electrode made of copper was glued by silver paint. The ferroelectric cathode was placed in a vacuum chamber evacuated by an oil-free vacuum system down to 3×10^{-5} Torr.

The driving pulse applied to the rear electrode of the sample was produced by a specially designed Blumlein generator. The generator produces an output pulse with an amplitude of $U_{\text{dr}} = 11\text{--}20$ kV on a matched load of 14Ω . When this driving pulse was applied to the ferroelectric cathode, the amplitude of the pulse decreased to $8\text{--}16$ kV with several oscillations. As was expected,^{5,12,13} similar results were obtained for both negative and positive driving pulses. However, for the positive driving pulse the intensity of the plasma formation was significantly lower. Therefore, in this article we will only present the data obtained for the negative driving pulse.

To study the profiles of spectral lines we used a Jobin-Yvon 750M spectrometer with a grating of 2400 grooves/mm and an aperture of $f = 1/6$. The spectral resolution of the spectrometer for an entrance slit width of $40 \mu\text{m}$ was $5.46 \text{ \AA}/\text{mm}$. The input and output optical systems were optimized for maximal light collection. The input optical system transfers the image of a plasma “slice” to the entrance slit of the spectrometer which has a width b and a height a . The magnification coefficient is determined by the maximal height of the plasma slice A_{max} which is limited by the diameter of the surface area covered by strips, $A_{\text{max}} = 70$ mm, and by the maximal opening of the entrance slit, $a_{\text{max}} = 20$ mm. For the chosen magnification of $M_{\text{in}} = 4$ we obtained the height of the plasma slice, $A = 68$ mm, and opening of the entrance slit $a = 17$ mm. Therefore, the width of the visible plasma slice can be determined as $B = bM_{\text{in}}$. For instance, for $b = 30 \mu\text{m}$ one obtains $120 \mu\text{m}$. In order to increase the efficiency of the light collection the focal length of the input lens should be decreased. The minimal focal length is determined by the minimal distance from the plasma to the lens which in our experimental setup is $f_1 = 50$ mm.

The output optical system focuses the image of the spectral line formed at the output of the spectrometer onto the

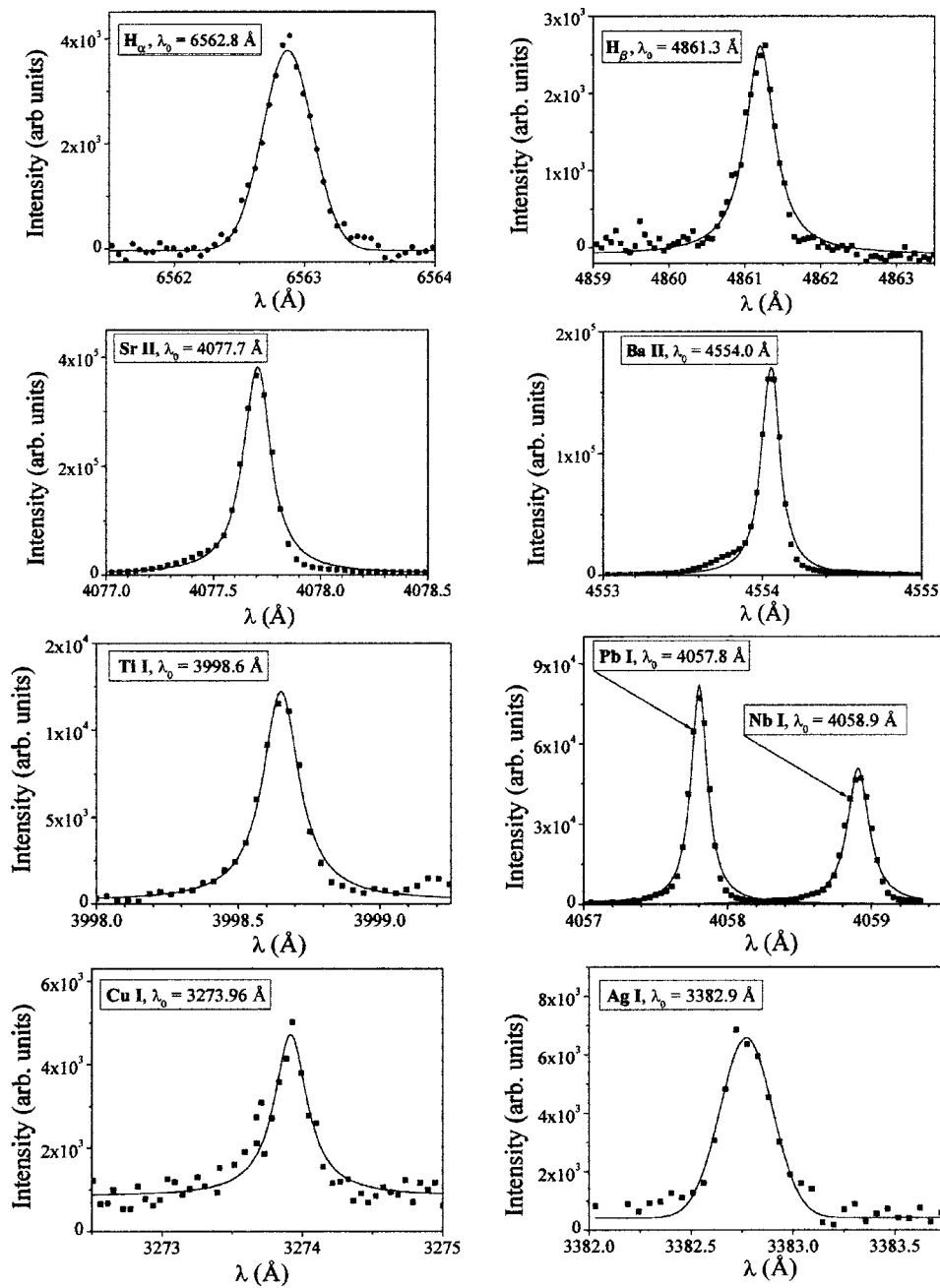


FIG. 2. Typical spectral line profiles observed within the first 100 ns at a distance of 0–0.05 mm from the ferroelectric surface. $\tau_{\text{frame}}=100$ ns, $U_{\text{dr}}=14$ kV.

photocathode of the 4Picos fast framing camera. The desired spectral resolution of the spectroscopic system is ≥ 0.05 Å/pixel. The camera has an equivalent pixel size of $27.4 \mu\text{m}$ that requires the magnification in the spectral plane (plane X) to be $M_{\text{out}X}=3$ in order to achieve the desired spectral resolution. This magnification was provided by an output biconvex lens with $f_2=75$ mm. However, the same magnification in plane Y , perpendicular to spectral plane X , leads to a spectral line height of $aM_{\text{out}X}=51$ mm, while the effective height of the photocathode of the 4Picos camera is only 15 mm. In order to avoid significant light losses in plane Y , an additional cylindrical lens with a focal length of 75 mm was used. This solution allowed us to achieve a spectral resolution of ~ 0.05 Å/pixel without light loss. Moreover, the focusing of the image in plane Y improves the signal-to-noise ratio of the observed image.

Alignment of the line of sight with respect to the front surface of the ferroelectric sample was performed using a HeNe laser. All optical components of the spectroscopic system were made of fused silica in order to provide a spectral range of 2000–7500 Å. The spectroscopic system was calibrated using a set of calibration lamps produced by Oriol.

III. EXPERIMENTAL RESULTS

A. Observation of temporal and spatial behavior of spectral line emission

Spectral lines of almost all the elements present in the ceramic composition were observed. Typical profiles of spectral lines, which were observed within the first 50 ns with respect to the beginning of the driving pulse at a distance of 0–0.05 mm from the front surface of the sample, are pre-

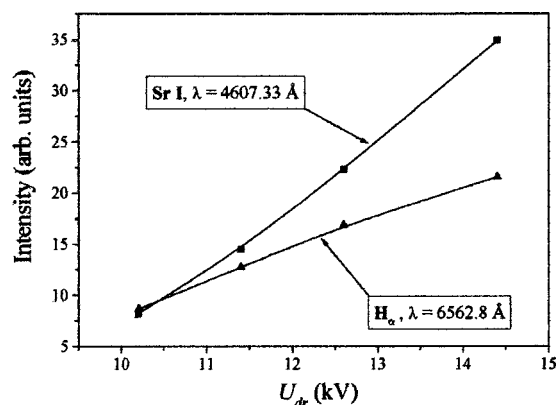


FIG. 3. Dependence of the spectral line intensity on the driving pulse amplitude (U_{dr}). A short duration negative driving pulse was applied to the rear electrode. $\tau_{frame}=50$ ns.

sented in Fig. 2. One can see that there is intense light emission from excited neutral atoms and ions even at the beginning of the driving pulse. This is direct proof that surface plasma forms almost simultaneously with application of the driving pulse. The observation of excited hydrogen atoms can be explained by the adsorbed surface monolayers, which include hydrogen atoms as well.¹⁶ Spectral light emission from excited copper neutrals and ions was also observed. The latter data showed that there is erosion of the strips on the front electrode. This erosion could be due to interaction of the discharge plasma with the strips as well as to explosive emission in the triple points. It is important to note that neither double ionized ions nor excited oxygen atoms and ions were observed. This indicates a relatively low temperature and density of the plasma electrons.

The intensity of the observed spectral lines was found to depend strongly on the driving pulse amplitude. That is, an increase of the amplitude of the driving pulse leads to an increase of the intensity of the spectral line emission. In Fig. 3 the dependence of the intensity of the spectral lines of H_{α} and SrI on the driving pulse amplitude is presented. These line intensities were obtained in time integrating mode (framing time of $5 \mu s$) 0.05 mm from the cathode surface. One can see that an increase of the amplitude leads to an almost linear increase of the line intensity. These data also agree with previous observations of light emission from the surface of ferroelectric cathodes, which showed an increase in the amount of surface discharges and their intensity with the increase of the amplitude of the driving pulse.¹² Also, the scaling obtained (see Fig. 3) agrees with the observed linear increase of the ion saturation current density measured by electrical probes.¹³ Indeed, the population of the excited levels, i.e., the intensity of the spectral line emission, depends linearly on the plasma density as well as on the plasma electron temperature. However, the latter is valid only for $T_e \ll (2-3)E_{ex}$, where E_{ex} is the excitation energy.²⁴

It was found that the intensity of the spectral lines follows the temporal behavior of the driving pulse. In Fig. 4 the temporal behavior of TiII and SrII spectral line intensity is presented. One can see that the maxima of the line emission intensity coincide with the maxima and minima of the ring-

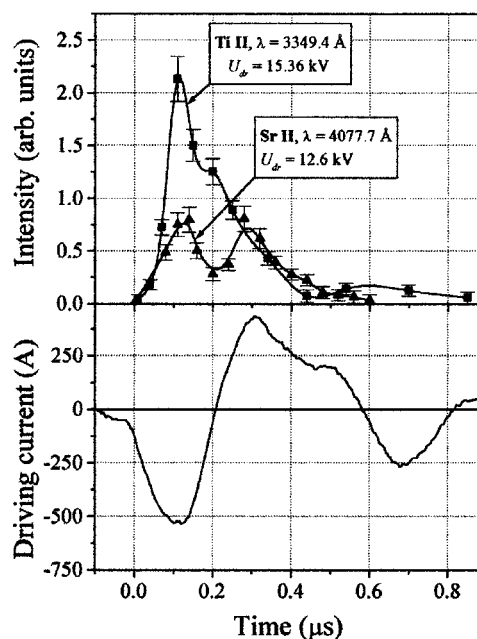


FIG. 4. Temporal behavior of the TiII and SrII spectral line intensities and the wave form of the driving current. $\tau_{frame}=50$ ns.

ing current of the driving pulse. One can speculate that the observed considerable rise in the line intensities with an increase in the driving current amplitude results from an increase of the plasma emitting area. Indeed, in the case of the flashover plasma, the latter serves as a dynamic electrode which increases its area with an increase of the driving current.⁵

The dependence of the H_{α} spectral line intensity versus the distance from the front surface of the ceramic sample is presented in Fig. 5. One can see fast decay of the intensity, that is, even at a distance of 1.5 mm the intensity decreases almost sevenfold compared with the observed intensity at a distance of 0.05 mm. The observed decrease in the spectral line intensity is faster than the density decrease measured by floating probes. It can be supposed that plasma cooling occurs together with a decrease in the plasma density.

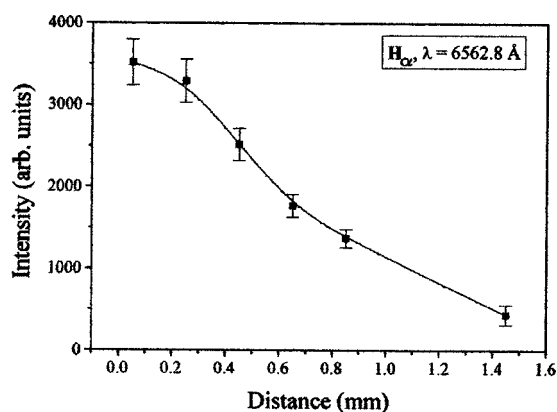


FIG. 5. Intensity of the H_{α} spectral line vs the distance from the front surface. $\tau_{frame}=5 \mu s$, $U_{dr}=13$ kV.

TABLE I. Measured broadening ($\Delta\lambda$) and the corresponding plasma ion temperature (T_i) for different spectral lines (λ) of elements with different atomic weights (A).

Element	TiI	TiI	SrII	NbI	BaII	PbI
A	47.9	47.9	87.6	92.9	137.3	207.2
$\lambda(\text{\AA})$	3998.7	4981.7	4077.7	4058.9	4554.0	4057.8
$\Delta\lambda(\text{\AA})$	0.03	0.034	0.027	0.028	0.02	0.012
	± 0.015	± 0.019	± 0.015	± 0.015	± 0.012	± 0.011
T_i (eV)	0.47	0.37	0.66	0.75	0.46	0.31
	± 0.12	± 0.12	± 0.2	± 0.22	± 0.16	± 0.26

B. Plasma ion temperature

The observed Doppler broadening of the emission lines was used for determination of the particle velocity distribution. Several emission lines of excited neutrals and ions were examined in order to obtain the dependence of the line broadening on the particle mass and charge. In addition, different emission lines of the same radiating atom or ion were examined in order to obtain the dependence of the line broadening on the wavelength. Thus, other mechanisms of line broadening can be excluded.

Based on the measurements carried out by single and double floating probes, the plasma density in the vicinity of the front surface was estimated as $n_e \approx 10^{13} - 10^{14} \text{ cm}^{-3}$ depending on the amplitude of the driving pulse.¹³ Also, taking into account the data obtained concerning the neutral flow formed as a result of surface flashover,^{23,25} one can estimate the neutral density as $n_n \approx 10^{20} - 10^{21} \text{ cm}^{-3}$ in a narrow (tens of microns) surface layer.^{6,16} Due to the high density of neutral atoms the ion-neutral equilibration time is less than 1 ns:

$$\tau_{in} \sim \frac{1}{n_n \langle \sigma_{in} V_{in} \rangle} \approx 10^{-10} \text{ s.}$$

Here $V_{in} \sim 10^6 \text{ cm/s}$ is the ion/neutral mean velocity, and $\sigma_{in} \sim 10^{-16} \text{ cm}^2$ is the cross section of ion-neutral collisions. Thus, the suggestion concerning the Maxwellian velocity distribution of ions and neutrals is reasonable. Further, fast plasma expansion occurs due to the large density gradients together with a respective decrease of the plasma density. This fast decrease of the plasma density does not allow electron-ion temperature equilibration on the time scale of

several tens of ns at distances $>0.5 \text{ mm}$ from the front surface of the ferroelectric. Indeed, one can estimate the equilibration time for electron-ion collisions as²⁶

$$\tau_{ie} \sim 3.7 \times 10^7 A \frac{T_e^{3/2}}{n_e} \geq 1 \text{ } \mu\text{s.}$$

Here $T_e \approx 3 \text{ eV}$ is the electron temperature, $n_e \sim 10^{14} \text{ cm}^{-3}$ is the electron plasma density, and A is the atomic weight.

The experimental data of the Doppler broadening of the spectral emission lines for different atoms and ions, as well as the estimate of the ion/neutral temperature, are presented in Table I. It was found that the Doppler broadening of the spectral lines scales according to the mass ratio and it increases linearly with an increase of the wavelength for the same charge state of the radiating atom or ion. One can see that the ion/neutral temperature is rather low and does not exceed 0.7 eV. In addition, it was found that the Doppler broadening does not depend on the distance from the front surface of the ferroelectric (see Fig. 6) nor on the amplitude of the driving voltage (see Fig. 7). These data agree well with the estimate of the equilibration time, which showed that the energy transferred to the ion/neutral plasma component from more hot electrons should be negligible within the time scale of several tens of ns.

C. Plasma electron temperature

The plasma electron temperature was determined by comparing the experimentally observed relative intensities of hydrogen (H_α and H_β) spectral lines with the calculated population ratio of these levels. One can expect the validity of the ‘‘corona’’ approximation for the expected plasma parameters. The corona model assumes a balance between collisional excitation processes and spontaneous radiative decay of the excited levels. Indeed, in our case for the levels of interest the Einstein coefficient is of the order of $10^7 - 10^8 \text{ s}^{-1}$ whereas the probability of electron impact de-excitation for $n_e = 10^{13}$ and $T_e = 3 \text{ eV}$ is smaller by a few orders.²⁷ For the plasma under study the collisional-radiative ionization rate²⁸ is smaller than $10^{-10} \text{ cm}^3/\text{s}$ and for $n_e = 10^{13} \text{ cm}^{-3}$ the estimated ionization time is $\sim 1 \text{ ms}$. Therefore for 500 ns our plasma does not reach ionization equilibrium and we have to do collision radiative (CR) modeling, as described in Ref. 29. This modeling takes into account not only the processes of electron impact excitation and spontaneous irradiation of selected energy levels, but also ionization and recombination processes. The plasma density and the plasma electron temperature were the input parameters of

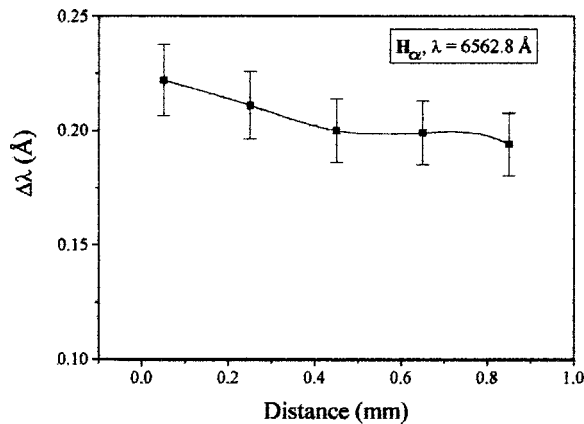


FIG. 6. Dependence of the measured broadening of the H_α line on the distance from the front surface of the sample. $\tau_{\text{frame}} = 5 \text{ } \mu\text{s}$, $U_{\text{dr}} = 13 \text{ kV}$.

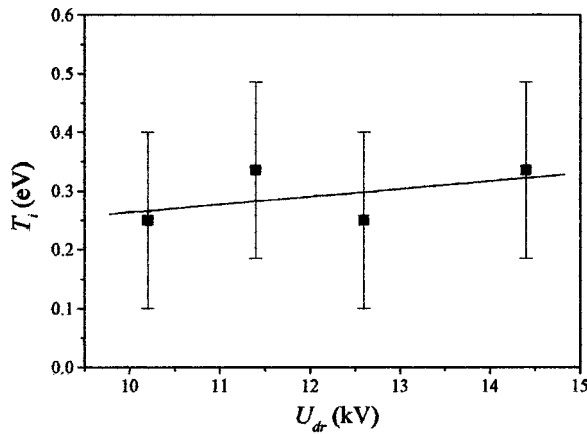


FIG. 7. Dependence of the plasma ion temperature on the driving pulse amplitude. $\tau_{\text{frame}}=5 \mu\text{s}$.

the calculations. It was assumed that the electrons have a Maxwellian velocity distribution, and that the plasma is optically thin. All hydrogen atoms were assumed to be in the ground state at the beginning of the process and there are no additional sources of hydrogen atoms in the observed plasma volume.

The results of the experiment and time dependent modeling are presented in Fig. 8. One can see that within the first 150 ns the population ratio is far from the steady state. Also, even after ~ 150 ns the population ratio still depends on the plasma density. This means that the corona approximation cannot be used at this time. Despite the presence of equilibrium between electron impact excitation and spontaneous irradiation, there is still no equilibrium between these processes and the ionization process. As was shown by time dependent CR modeling, this equilibrium is reached only ~ 1 ms after the beginning of the process.

The best fit of the measured and calculated population ratios was obtained at $T_e=3$ eV (see Fig. 8). The plasma density reaches $2 \times 10^{12} \text{ cm}^{-3}$ at $t \sim 300$ ns. These results are in satisfactory agreement with the measurements with electrical probes.¹³

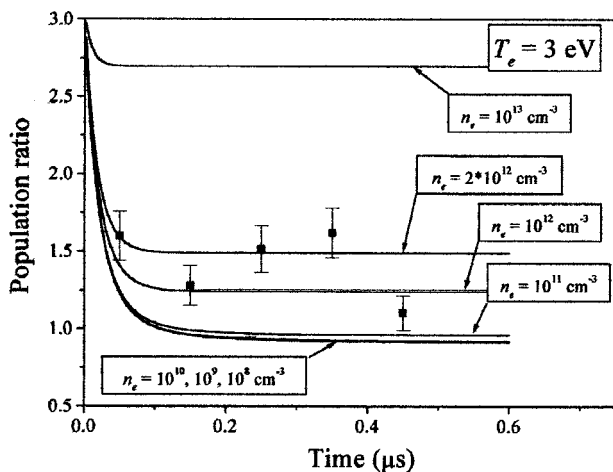


FIG. 8. Measured ratios of the H_α and H_β spectral line intensities and calculated population ratios for $T_e=3$ eV and different plasma electron densities.

D. Plasma electron density

Stark broadening of H_α and H_β spectral lines was used for estimation of the plasma density. As is well known these Balmer series transitions are sensitive to the linear Stark effect.²⁹ A remarkable feature of the physical process investigated is that the Stark effect can be induced not only by ion electric microfields (the quasistatic approximation) and by fast changing electron microfields (the impact approximation) but also by the electric field induced by the noncompensated surface polarization charges. The latter can be assumed to be a quasistatic electric field, which should lead to splitting of the spectral line to Stark components. The estimated full width at half maximum (FWHM) of the H_β spectral line, when affected by quasistatic electric fields of ions with a density of $n_i \sim 10^{13} - 10^{14} \text{ cm}^{-3}$ in the absence of external electric fields, is $\Delta\lambda \sim 0.1 - 0.43 \text{ \AA}$. However, the appearance of an external electric field $E_{\text{ext}} \sim 10^4 \text{ V/cm}$, which could be induced by noncompensated surface polarization charges, should lead to spectral line splitting of $\Delta\lambda \sim 5.3 \text{ \AA}$. Here the relation between plasma density and electric field is determined by the Holtsmark distribution.²⁸ Thus, careful treatment of hydrogen spectral lines could provide information about the plasma density and about the existence of electric fields of surface polarization charges.

Typical examples of H_α and H_β spectral line profiles are presented in Fig. 2. An analysis of the spectral lines was done after deconvolution of the instrumental and Doppler thermal broadening which were obtained from calibration and observation of spectral lines which are nonsensitive to Stark broadening (see Table I). It was found that the observed Stark broadening is almost of the order of the accuracy of the measurements. Thus, one can estimate the plasma density as $\leq 10^{13} \text{ cm}^{-3}$.^{30,31}

The absence of significant broadening of H_α and H_β spectral lines is direct proof of the absence of electric fields larger than 10^3 V/cm at a distance several tens of μm from the front surface of the ferroelectric. This coincides well with the model of plasma formation which predicts screening of the electric fields of polarization surface charges by the charged plasma particles.

IV. SUMMARY

We carried out spectroscopic measurements of the plasma formed on the front surface of a ferroelectric sample upon the application of a driving pulse. Our recent observations¹² of visible light emission from the surface of ferroelectric samples showed that this plasma formation occurs independent of the composition and polarization state of the ferroelectric samples, as well as of the polarity of the driving pulse. Therefore, we believe that the spectroscopic data we have obtained are relevant also for cases of other ferroelectrics subjected to high-voltage driving pulses of nanosecond pulse duration.

By spectroscopic diagnostics it was shown that the plasma formation occurs within the first 50 ns of the beginning of the driving pulse. The plasma consists of the atoms and ions of the ferroelectric material, as well as of the material of the front electrode. The latter indicates the presence of

an erosion process of the electrode material. This erosion could be either due to an explosive emission process or due to interaction of the plasma particles with the electrode.

It was found that the parameters of the plasma depend strongly on the amplitude of the driving pulse. Namely, the larger the amplitude of the driving pulse the larger the observed intensity of spectral line emission. The plasma obtained is rather cool: the electron and ion temperatures do not exceed 3 and 0.6 eV, respectively. Also, it was shown that the plasma density 1 mm from the front surface does not exceed 10^{12} cm^{-3} .

We did not observe any large quasistatic electric fields that clearly showed the absence of a large ($> 10^3 \text{ V/cm}$) electric field which can be induced by the appearance of the noncompensated surface polarization charges. In the case of the surface plasma formation initiated in the triple points, the plasma expands along the surface of the ferroelectric. Therefore, the plasma serves as a dynamic electrode because the plasma supplies charged particles that screen the electric field of the noncompensated surface polarization charges.

¹H. Riege, Nucl. Instrum. Methods Phys. Res. A **340**, 80 (1994).

²H. Gundel, in *Proceedings of the NATO Advanced Research Workshop on Science and Technology of Electroceramic Thin Films* (Kluwer Academic, Dordrecht, The Netherlands, 1994), pp. 335–351.

³C. B. Fleddermann and J. A. Nation, IEEE Trans. Plasma Sci. **25**, 212 (1997).

⁴H. Riege, I. Boscolo, J. Handerek, and U. Herleb, J. Appl. Phys. **84**, 1602 (1998).

⁵G. Rosenman, D. Shur, Ya. E. Krasik, and A. Dunaevsky, J. Appl. Phys. **88**, 6109 (2000), and references therein.

⁶G. A. Mesyats, *Explosive Electron Emission* (URO, Ekaterinburg, Russia, 1998).

⁷A. Dunaevsky, Ya. E. Krasik, J. Felsteiner, and S. Dorfman, J. Appl. Phys. **85**, 8474 (1999).

⁸H. Gundel, H. Riege, E. J. N. Wilson, J. Handerek, and K. Zioutas, Nucl. Instrum. Methods Phys. Res. A **280**, 1 (1989).

⁹V. D. Kugel, G. Rosenman, D. Shur, and Ya. E. Krasik, J. Appl. Phys. **78**, 2248 (1995).

¹⁰D. Shur, G. Rosenman, Ya. E. Krasik, and V. D. Kugel, J. Appl. Phys. **79**, 3669 (1996).

¹¹G. Rosenman, D. Shur, Kh. Garb, R. Cohen, and Ya. E. Krasik, J. Appl. Phys. **82**, 772 (1997).

¹²Ya. E. Krasik, A. Dunaevsky, and J. Felsteiner, J. Appl. Phys. **85**, 7946 (1999).

¹³A. Dunaevsky, Ya. E. Krasik, J. Felsteiner, and S. Dorfman, J. Appl. Phys. **85**, 8464 (1999).

¹⁴S. P. Bugaev and G. A. Mesyats, Sov. Phys. Dokl. **16**, 41 (1971).

¹⁵V. F. Puchkarev and G. A. Mesyats, J. Appl. Phys. **78**, 5633 (1995).

¹⁶H. C. Miller, IEEE Trans. Electr. Insul. **24**, 765 (1989).

¹⁷N. J. Shannon, P. W. Smith, P. J. Dobson, and M. J. Shaw, Appl. Phys. Lett. **70**, 1625 (1997).

¹⁸W. Zhang and W. Huebner, J. Appl. Phys. **83**, 6034 (1998).

¹⁹G. Benedek, I. Boscolo, J. Handerek, and H. Riege, J. Appl. Phys. **81**, 1396 (1997).

²⁰W. Zhang, W. Huebner, S. E. Sampayan, and M. L. Krogh, J. Appl. Phys. **85**, 8495 (1999).

²¹S. P. Bugaev, A. M. Iskol'dskii, and G. A. Mesyats, Sov. Phys. Tech. Phys. **12**, 1358 (1968).

²²S. P. Bugaev, V. V. Kremnev, Yu. I. Terent'ev, V. G. Shpak, and Ya. Ya. Yurike, Sov. Phys. Tech. Phys. **16**, 1547 (1972).

²³A. Dunaevsky, Ya. E. Krasik, J. Felsteiner, S. Dorfman, A. Berner, and A. Sternlieb, J. Appl. Phys. **89**, 4480 (2001).

²⁴B. Chapman, *Glow Discharge Processes* (Wiley, New York, 1980).

²⁵F. F. Chen, *Introduction to Plasma Physics and Controlled Fusion* (Plenum, New York, 1974).

²⁶N. A. Krall and A. W. Trivelpiece, *Principle of Plasma Physics* (McGraw-Hill, New York, 1973).

²⁷K. M. Aggarwal, K. A. Berrington, P. G. Burke, A. E. Kingston, and A. Pathak, J. Phys. B **24**, 1385 (1991).

²⁸H. R. Griem, *Plasma Spectroscopy* (McGraw-Hill, New York, 1964).

²⁹Yu. V. Ralchenko and Y. Maron, J. Quant. Spectrosc. Radiat. Transf. **71**, 609 (2001).

³⁰E. W. Weber, R. Frankenberger, and M. Schilling, Appl. Phys. B: Photophys. Laser Chem. **B32**, 63 (1983).

³¹H. R. Griem, Contrib. Plasma Phys. **40**, 46 (2000).